Proceedings of the ASME 2022
International Mechanical Engineering Congress and Exposition
IMECE2022
October 30-November 3, 2022, Columbus, Ohio

IMECE2022-95790

THERMAL ANALYSIS AND DESIGN OF SELF-HEATING MOLDS USING LARGE-SCALE ADDITIVE MANUFACTURING FOR OUT-OF-AUTOCLAVE APPLICATIONS

Deepak Kumar Pokkalla[1], Ahmed Arabi Hassen[1], Jesse Heineman[1], Thomas Snape[2], John Arimond[2], Vlastimil Kunc[1], Seokpum Kim[1,*]
[1]Manufacturing Science Division, Oak Ridge National Laboratory, Knoxville, TN, USA
Advanced Structures and Composites Center, University of Maine, Orono, ME, USA
[*]Corresponding author: kimsp@ornl.gov

ABSTRACT

Autoclave processing is a commonly used state-of-the-art fiber-reinforced composite manufacturing technology, albeit with high capital cost, long cycle times and high energy consumption. Alternatively, out-of-autoclave processing reduces the initial and operating costs while producing composite structures with similar quality as that of autoclave parts. Additive Manufacturing (AM) the scaled-up molds for out-of-autoclave process using carbon fiber (CF) reinforced composite offers design flexibility, enhanced mechanical, and thermal properties in addition to reduction in weight and cost. However, heating of these molds using an oven is still expensive and necessitates an energy-efficient heating process. In this study, resistive heating through heating elements embedded within fiber reinforced composite molds is used as an efficient heating mechanism. The goal is to design wire embeddings and determine the optimal heat flux density to achieve a target uniform temperature of 80^0C across the mold surface. To this end, numerical analyses were performed to evaluate the temperature distribution across the composite mold surface for a given wire placement and mold configuration. Constant thermal properties of the 20 wt.% short CF reinforced acrylonitrile butadiene styrene (ABS) were used in the thermal analysis. Time taken to reach the steady state temperature was also estimated. Design guidelines for wire embeddings were included to enable efficient manufacturing of fiber-reinforced composites through out-of-autoclave molds.

Keywords: Large Scale Additive Manufacturing, Carbon-fiber reinforced composites, 3D Printing, Heat Transfer, Thermal Analysis, Wire embedding, Out-of-autoclave Manufacturing, Composite Mold.

NOMENCLATURE

C_p	Specific heat
$\kappa(\kappa_1, \kappa_2, \kappa_3)$	Thermal conductivity (in x, y, and z direction)
q	Local heat flux density
T	Temperature
t	time
h	convection coefficient
h_g	contact conductance

1. INTRODUCTION

Additive manufacturing of fiber reinforced polymer composites has been the subject of increased interest in recent years as it enables fabrication of lightweight and high-performance structures. The design flexibility of AM processes opens avenues to manufacture parts for a wide range of applications in automotive, renewable energy, and aerospace manufacturing industries [1-5]. Parts for end use applications such as aerial vehicle's components, boat hull, rapid prototyping tool, and engine bracket can be readily available by 3D printing them directly [6]. In addition, parts for molding or tooling applications such as autoclave molds can be manufactured indirectly [7]. Considering that the properties of the AM parts are

limited due to inherent porosity and lesser strength in the build direction, indirect fabrication of parts such as autoclave molds has received significant attention due to their industrial applications. The AM process provides design freedom, enables a greater choice of materials, and allows scalability; thus, it is greatly appreciated by the mold and dies industry.

The traditional state-of-the-art autoclave process for fiber-reinforced polymer composite manufacturing is limited due to high capital and labor costs, long cycle times, inefficient conduction heating and high energy absorption. Although an alternative out-of-autoclave processing resolves some issues, there are still major challenges for polymer composite manufacturing such as cost of materials, machining of molds and inefficient heating process. To overcome challenges involved in fabrication of scaled-up molds, large scale material extrusion additive manufacturing has been increasingly used [5, 6, 8]. Oak Ridge National Laboratory (ORNL) successfully fabricated the autoclave molds made up of fiber-reinforced thermoplastic-based composites using Big Area Additive Manufacturing (BAAM) [6, 8]. The use of BAAM to fabricate autoclave molds significantly reduced the cost by 10-100 times and entire cycle time from months to weeks proving to be a viable energy-efficient manufacturing solution.

Despite manufacturing molds using BAAM, the autoclave process is limited due to inefficient heating and requires a large room-sized oven driving up the cost of high-performance composite parts. An innovative heating strategy by embedding heating elements within a mold was developed recently to eliminate the necessity of oven and decreasing the cycle time [9]. The BAAM is integrated with a wire co-extrusion tool to enable embedding of a resistive heating wire such as nichrome wire within the printed bead. The details of the wire co-extrusion tool design and integration with BAAM was presented in [10]. The embedded wire within the part heats up the mold efficiently using the Joule heating principle and via conduction in contrast to oven-based heating used for composite curing. However, the challenge to use this innovative heating process lies in efficient design of wire embeddings for a given mold configuration and choice of materials to achieve a uniform target mold surface temperature. Without a proper design, cold spots may arise due to large spacing between the embedded wires and/or unwanted localized heating may occur if the embedded wires are too close.

The present study focuses on designing additive manufactured shell mold with co-extruded wires. A numerical model for the AM part with co-extruded wire was developed to evaluate various design configurations. The time taken to reach steady state temperature will also be estimated. Wire embeddings with different spacing for a given depth are considered. The heat flux density required to achieve the uniform target temperature on the mold surface is estimated by evaluating various designs using the developed numerical model. The focus of this work is to perform thermal analysis and design the shell mold made up of three different subcomponents. The spatial distance between the embedded wires, depth of the wires from the top mold surface, and heat flux density are the critical factors affecting the temperature profile on the mold surface. Determining the optimal values for these critical parameters is necessary to allow uniform curing and solidification during the autoclave process. Otherwise, undesired localized heating resulting in melting or deforming the mold and/or unwanted cold spots may occur during the composite manufacturing. The numerical analysis and design investigation here presents a systematic study to evaluate thermal behavior and design additively manufactured wire embedded molds for energy efficient out-of-autoclave applications.

2. NUMERICAL MODELLING

In this section, the details of the numerical model and design criteria for additively manufactured shell mold with co-extruded wires are elaborated.

2.1 Mold Manufacturing

The shell mold considered in this study is made up of three subcomponents with different materials as shown in Fig. 1. The spatial distance between the embedded wires and depth of the wires from the top mold surface are denoted by s and d as illustrated in Fig. 1.

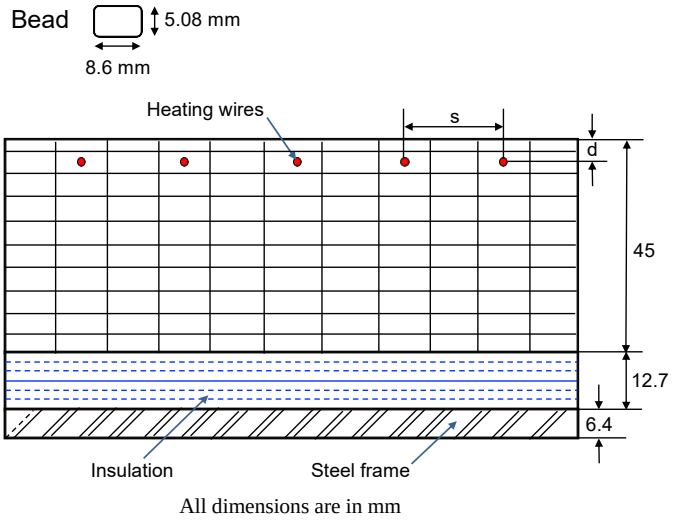

FIGURE 1: SCHEMATIC OF ADDTIVELY MANUFACTURED SHELL MOLD WITH CO-EXTRUDED WIRES

The top portion of the mold is a layer of 45 mm consists of 20 wt% carbon fiber reinforced acrylonitrile butadiene styrene (ABS/CF20) with embedded nichrome 26 AWG wires. Here, ABS/CF20 is chosen as a polymer composite material due to its common use in large scale AM technologies. The material properties of ABS/CF20 have been analyzed in an earlier study [11-15]. Nichrome wires were chosen as heating elements in this

study as they are commonly used for resistive heating in various applications. The wires had a diameter of 0.4 mm. During the extrusion process, the fibers in ABS/CF20 are extruded with preferential orientation along the deposition direction. In the BAAM system at ORNL, the extruded material is flattened by tamper immediately after extrusion and thus the thermal conductivity of the material is anisotropic. The middle portion of the mold is made up of 12.7 mm layer of insulation material with relatively low thermal conductivity. The bottom of the mold consists of a 6.4 mm steel base plate. The thermal properties of various constituent materials are listed in Table 1. The thermal properties of nichrome are an average of the minimum and maximum values listed in [15]. The steel thermal properties are obtained from [16].

TABLE 1: THERMAL PROPERTIES OF MOLD MATERIALS

		ABS/CF20	Nichrome	Insulation	Steel
Heat Capacity (J/Kg K)	C_p	1225	440	1100	466
Thermal conductivity (W/m K)	κ_1	1.124	12.5	0.02	45
	κ_2	0.434	12.5	0.02	45
	κ_3	0.244	12.5	0.02	45
Emissivity		0.95			0.2

For manufacturing the composite mold, multiple layers of ABS/CF20 will be deposited on top of the insulation to create the heating panel. The resistive wire will be co-extruded to be at the center of the bead in a 3D printed mold. The top surface of the 3D printed mold needs to be machined to remove the rough and wavy surface generally seen in the build (height) direction. To achieve a smooth mold surface for composite manufacturing half of the bead will be machined off from the top surface after printing.

For composite manufacturing using the wire embedded mold, the wires at both ends of the printed panel are connected to a power supply. Upon supplying electricity, heat generated from the wires within beads transfers to the top surface of the mold. The heat flux density through these wires corresponding to a chosen values of spacing and depth needs to be determined such that the top mold surface temperature reaches approximately 80^0 C at steady state. The design criteria also include restricting the maximum temperature within the mold to roughly 130^0 C. Given this mold configuration and design criteria, numerical analysis needs to be performed to determine the optimal spacing and depth parameters while minimizing the time taken to reach the steady state temperature.

2.2 Simulation Setup

A numerical model is developed for the heat transfer analysis of self-heating mold with embedded wires using Abaqus, a commercial finite element analysis (FEA) software. The heat transfer analysis was performed on different mold designs using finite element method (FEM) to investigate the transient and steady-state heating processes [17]. For the additive manufacturing of self-heating molds, the BAAM 3D-printing machine was equipped with a wire coextrusion tool [9]. The wires are co-extruded with the material through a coextrusion nozzle and thus the wires are placed at the center of the bead while being extruded. Considering this, several design configurations are possible for AM self-heating mold by changing the parameters such as spacing and depth of wires along with heat flux density. However, preliminary analysis revealed that higher values of depth would necessitate increased heat flux density through the wire to achieve the target surface temperature but violates the design requirement for maximum temperature of the mold (130^0 C). Hence, two different depths of 5 mm and 10 mm from the top mold surface are considered for the wire embedding in the subsequent analysis.

Two different spacings were chosen for the numerical study based on the bead dimensions and the above depths for wire embedding: (i) wire embedding with a spacing of 8.6 mm, and (ii) wire embedding with a spacing of 17.2 mm, as illustrated in Fig. 2. The numerical analysis was performed on cross-section of the repeating unit in Fig. 2. For each design in Fig. 2, the corresponding cross sections are represented in Fig. 3. The left and right surfaces of each design are the boundary surfaces of symmetry.

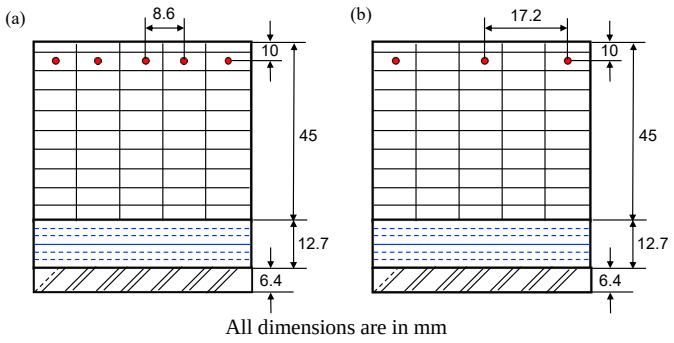

FIGURE 2: TWO DESIGNS FOR THE WIRE EMBEDDED MOLDS. (a) WIRE EMBEDDED IN ADJACENT BEADS (NO SKIPPING), (b) WIRE SKIPPING EVERY OTHER BEAD.

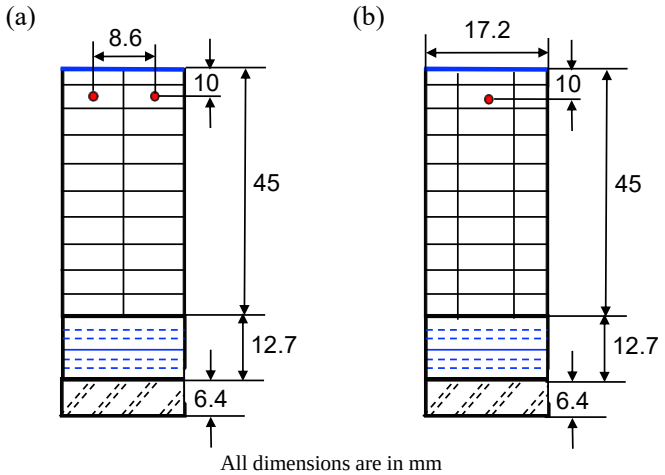

FIGURE 3(a-b): CROSS SECTIONS OF THE REPEATING UNIT FOR NUMERICAL SIMULATIONS REPRESENTING TWO CASES SHOWN IN FIGURE 2. THE RED CIRCLE IN THE CENTER REPRESENTS THE WIRE.

The numerical simulation is performed using a commercial FEM package, Abaqus by Dassault Systems. The constitutive relations utilized for the heat transfer simulations are thermal conduction in the form of Fourier's law (Eq. 1), the convection as per the Newton's law of cooling (Eq. 2), and the thermal radiation using Stephan-Boltzmann law (Eq. 3) and are given below:

$$\frac{dq}{dt} = -\kappa \nabla T \quad (1)$$

$$\frac{dq}{dt} = h(T - T_0) \quad (2)$$

$$q = \sigma A T^4 \quad (3)$$

where, q is the local heat flux density, κ is the conductivity, ∇T is the temperature gradient, h is the convection coefficient, and is the environment temperature. The conductivity of polymer composite is an anisotropic property and thus different values of conductivity given by κ_1, κ_2, and κ_3 in Table 1 corresponding the directions of deposition, width, and height, respectively, are used in the numerical simulations. The boundary conditions applied on the repeating unit are depicted in Fig. 4. The convection was applied on the top and bottom surfaces while the left and right surfaces are assumed to be adiabatic due to the symmetry.

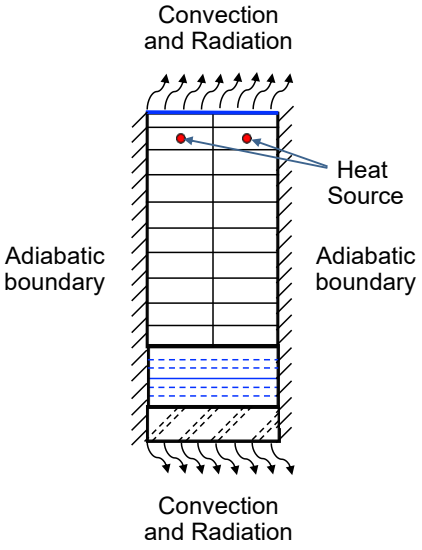

FIGURE 4: APPLIED BOUNDARY CONDITIONS FOR THE SIMULATION. THE LEFT AND RIGHT BOUNDARIES ARE ASSUMED TO BE ADIABATIC. CONVECTION AND RADIATION ARE APPLIED AT THE TOP AND BOTTOM BOUNDARIES.

The finite element analyses on the repeating units using above boundary conditions were performed in Abaqus using 10-node quadratic heat transfer tetrahedron (DC3D10) elements. The mesh size is chosen to be sufficiently small to ensure the temperature profile obtain for a given heat flux is independent of mesh. A mesh size of 0.2 mm is used for the CF/ABS mold, insulation zone, and steel frame. A fine mesh size of 0.01 mm is used for the nichrome wire of 0.4 mm diameter. The interface between the layers is assumed to be perfect in this study. Also, the interfaces between different materials are modeled using surface to surface contact in Abaqus with a high conductance (1000 W/m^2 K).

The aim is to determine the optimal layout of wires to achieve a target temperature of 80^0 C across the top surface (represented by a green line in Fig. 4) using resistive heating of the embedded wire. In this study, a gap conductance of 1000 W/m^2 K is used for the interfaces as the current study focuses on providing preliminary design guidelines for the effect of spacing and depth on the temperature profile at the steady state. In practice, temperature drops and a discontinuity in the temperature profile can be seen by considering the imperfection or a contact resistance between the layers [18]. Modeling the effect of contact resistance by using a lower value for gap conductance of 30 W/m^2 K illustrates that temperature drops at the discontinuity and a greater disparity is observed at the top mold surface. The interfacial effects between layers and different materials for the presented mold configurations can be evaluated using the proposed model by merely changing the gap conductance at the interface.

3. RESULTS AND DISCUSSION

In this section, the developed numerical model is utilized to design the self-heating mold to achieve a uniform target surface temperature while satisfying the other design requirements.

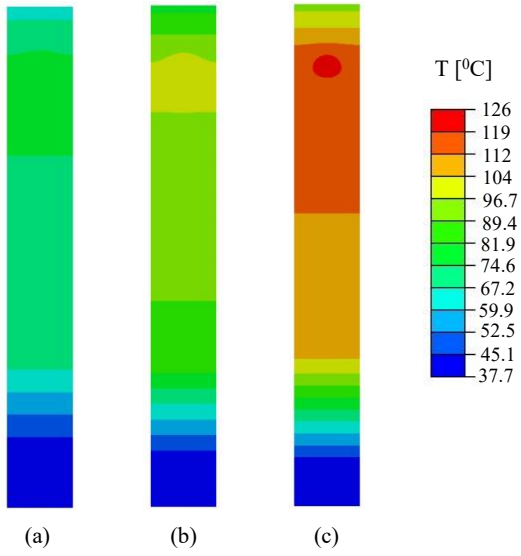

FIGURE 5(a-c): TEMPERATURE DISTRIBUTION AT THE LAST TIME STEP (t = 27.8 hours) FOR DIFFERENT HEAT GENERATION VALUES (q = 4 W/m, 6 W/m, and 8 W/m) WITH A WIRE SPACING OF 8.6 mm AND DEPTH OF 5 mm.

Heat transfer simulations were performed for the four different mold designs of which two designs with a depth of 10 mm are shown in Fig. 3. The prescribed boundary conditions are depicted in Fig. 4. The wires are embedded at a depth of 5 mm and 10 mm from the top surface as determined by the prior numerical analysis. The heat generation values ranging from 6 W/m to 10 W/m for a spacing of 8.6 mm and 12 W/m to 18 W/m for a spacing of 17.2 mm were used in simulations for repeating unit designs to determine an optimal heat input such that the top mold surface reaches roughly 80^0 C. The total heat generation for the entire panel design shown in Fig. 2 can be calculated based on the optimal heat flux density and the cross-sectional dimensions of the repeating units.

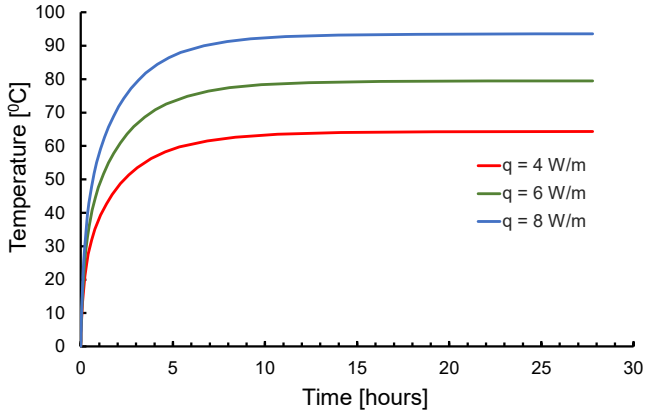

FIGURE 6: TEMPERATURE HISTORY AT THE FURTHEST POINT FROM THE HEAT SOURCE (WIRE) FOR DIFFERENT HEAT GENERATION VALUES (q = 4 W/m, 6 W/m, and 8 W/m) WITH A WIRE SPACING OF 8.6 MM AND DEPTH 5 mm. FOR ALL CASES, TEMPERATURE REACHES A STEADY STATE AT t = 8 HOURS.

The temperature distributions of the design with 8.6 mm spacing and depths of 5 mm and 10 mm at the steady state for different heat generation values are shown in Figs. 5 & 7.

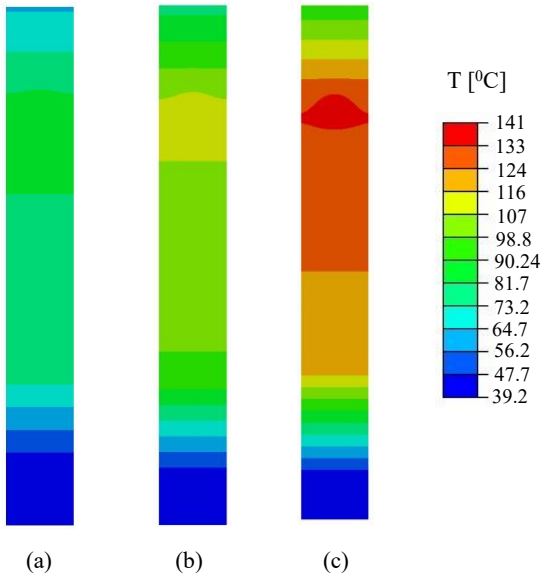

FIGURE 7(a-c): TEMPERATURE DISTRIBUTION AT THE LAST TIME STEP (t = 27.8 hours) FOR DIFFERENT HEAT GENERATION VALUES (q = 4 W/m, 6 W/m, and 8 W/m) WITH A WIRE SPACING OF 8.6 mm AND DEPTH OF 10 mm.

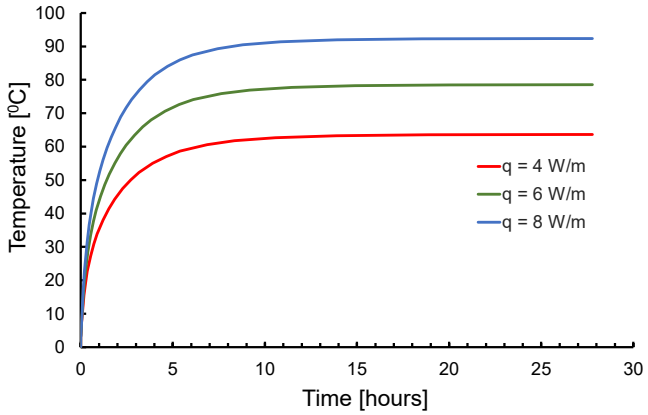

FIGURE 8: TEMPERATURE HISTORY AT THE FURTHEST POINT FROM THE HEAT SOURCE (WIRE) FOR DIFFERENT HEAT GENERATION VALUES (q = 4 W/m, 6 W/m, and 8 W/m) WITH A WIRE SPACING OF 8.6 MM AND DEPTH 10 mm. FOR ALL CASES, TEMPERATURE REACHES A STEADY STATE AT t = 8 HOURS.

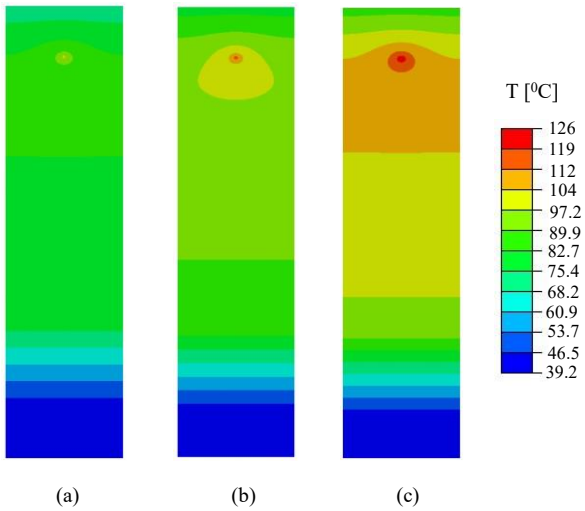

FIGURE 9(a-c): TEMPERATURE DISTRIBUTION AT THE LAST TIME STEP (t = 27.8 hours) FOR DIFFERENT HEAT GENERATION VALUES (q = 4 W/m, 6 W/m, and 8 W/m) WITH A WIRE SPACING OF 17.2 mm AND DEPTH OF 5 mm.

The temperature history at the corner on the surface located at furthest point from the wire is computed for different input heat flux densities as depicted in Figs. 6 & 8. For all these cases, the surface temperature reaches a steady state at around t = 8 hours. The temperature profile of the mold surface at the steady state is uniform throughout the width as can be seen in Figs. 5 & 7. The top mold surface steady state temperature for a depth of 5 mm 8.6 mm and heat generation values of 4 W/m, 6 W/m, and 8 W/m were computed as 62.6^0 C, 77.5^0 C and 91.3^0 C. Similarly, for the mold configuration with wire depth of 10 mm, the mold surface temperatures were computed as 61.7^0 C, 75.85^0 C and 90.5^0 C. Hence, the optimal wire layout within the mold to achieve a uniform target temperature of 80^0 C at the top mold surface is determined as depth of 5 mm, spacing of 8.6 mm and heat of 6 W/m.

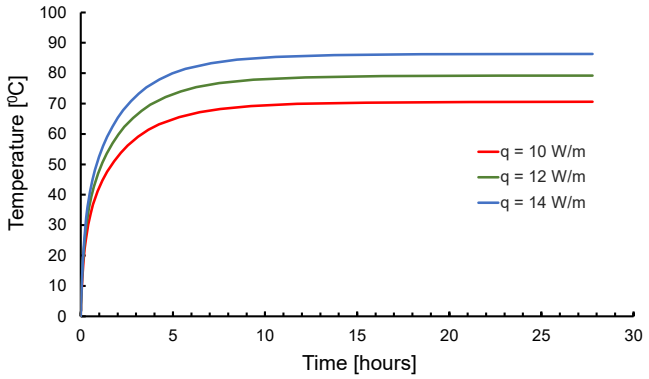

FIGURE 10: TEMPERATURE HISTORY AT THE FURTHEST POINT FROM THE HEAT SOURCE (WIRE) FOR DIFFERENT HEAT GENERATION VALUES (q = 4 W/m, 6 W/m, and 8 W/m) WITH A WIRE SPACING OF 17.2 MM AND DEPTH 5 mm. FOR ALL CASES, TEMPERATURE REACHES A STEADY STATE AT t = 8 HOURS.

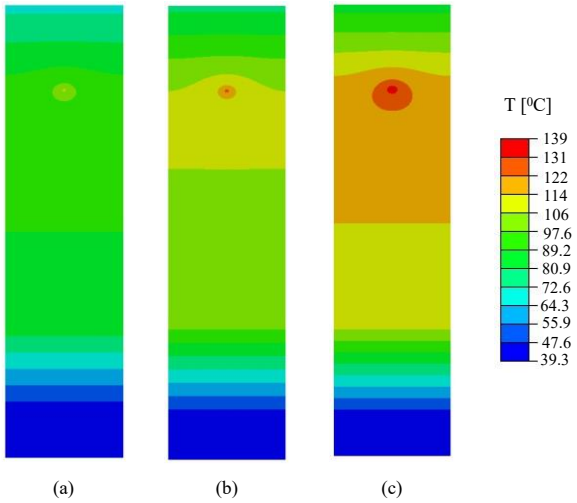

FIGURE 11(a-c): TEMPERATURE DISTRIBUTION AT THE LAST TIME STEP (t = 27.8 hours) FOR DIFFERENT HEAT GENERATION VALUES (q = 4 W/m, 6 W/m, and 8 W/m) WITH A WIRE SPACING OF 17.2 mm AND DEPTH OF 10 mm.

Furthermore, simulations were performed for a spacing of 17.2 mm, depths of 5 mm and 10 mm and various heat generation values of 10 W/m, 12 W/m, and 14 W/m to determine other set of optimal design parameters. The temperature distributions across the cross-section of the repeating units for different depths of wire embeddings are shown in Figs. 9 & 11. The temperature history at the corner on the surface located at furthest point from the wire is computed for different input heat flux densities and depths as shown in Fig. 10 & 12. The surface temperature for all these cases reaches a steady state at around t = 9 hours, an hour longer than the previous case with a spacing of 8.6 mm. The temperature of the top mold surface at steady state is uniform the width as can be seen in Figs. 9 & 11. The top mold surface steady state temperature for a depth of 5 mm and heat generation values of 10 W/m, 12 W/m, and 14 W/m were computed as 69.2^0 C, 77.8^0 C and 84.5^0 C. Similarly, for the mold configuration with wire depth of 10 mm, the mold surface temperatures were computed as 68.4^0 C, 76.4^0 C and 83.8^0 C.

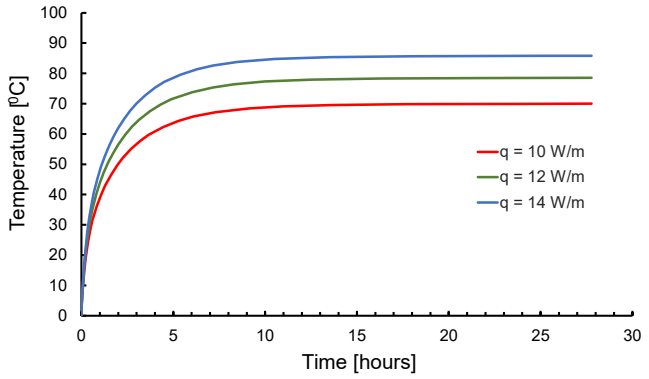

FIGURE 12: TEMPERATURE HISTORY AT THE FURTHEST POINT FROM THE HEAT SOURCE (WIRE) FOR DIFFERENT HEAT GENERATION VALUES (q = 4 W/m, 6 W/m, and 8 W/m) WITH A WIRE SPACING OF 17.2 MM AND DEPTH 10 mm. FOR ALL CASES, TEMPERATURE REACHES A STEADY STATE AT t = 8 HOURS.

Thus, the optimal wire layout to achieve a uniform target temperature of 80^0 C at the top mold surface is determined a spacing of 17.2 mm and a heat of 12 W/m for a depth of 5 mm. Moreover, the developed model can be directly used to study the effect of interfaces between different materials and gaps between different 3D printed layers on the temperature profile of the AM mold by tuning gap conductance values.

The study here considered repeating units for heat transfer analysis and design of wire embeddings. However, during a design of self-heating mold with a prescribed geometry, a coupled thermo-mechanical analysis is necessary. First, thermal history for the heating of the entire self-heating mold is extracted from heat transfer analysis. Using the thermal history, a structural analysis is subsequently performed to determine the deformation and dimensional integrity of the mold design. In this study, thermal analysis is performed only on repeating units and thus, thermo-mechanical analysis is not included here. In addition to rectilinear wire placements, 2D curvilinear layouts of the wire embedding can be determined using optimization algorithms such as sensitivity analysis [17, 19] or genetic algorithm [20] for self-heating molds with complex geometries.

4. CONCLUSION

The performance of additively manufactured shell molds with co-extruded wires have been evaluated by performing heat transfer analysis on the test panel designs. Four different spatial configurations for the mold with different spacing between the wires and depth from the top mold surface are considered as potential candidates based on preliminary analyses. Assuming a negligible contact resistance between the printed layers of the polymer composite in the build direction, the optimal heat generation values for the four different spatial configurations were determined through the numerical simulations. With the optimal heat generation values, a uniform temperature of 80^0 C on the mold surface with a maximum disparity within 1^0 C was obtained. The corresponding maximum temperature of the mold was around 130^0 C satisfying the design criteria. The presented analysis and design provide a guideline for manufacturing self-heating mold in terms of spacing and depth of wire embeddings. Such a design of self-heating molds is critical to eliminate the need for a room-sized oven for composite curing during out-of-autoclave process.

ACKNOWLEDGEMENTS

This research is sponsored by the US Department of Energy (DOE), Office of Energy Efficiency and Renewable Energy, Advanced Manufacturing Office, under contract DE-AC05-00OR22725 with UT-Battelle LLC.

REFERENCES

[1] C. B. Williams and R. Ilardo, “Design and manufacture of a Formula SAE intake system using fused deposition modeling and fiber-reinforced composite materials,” *Rapid Prototyp. J.*, vol. 16, no. 3, pp. 174–179, 2010.

[2] S. L. Marasso et al., *et al.*, “PLA conductive filament for 3D printed smart sensing applications,” *Rapid Prototyp. J.*, vol. 24, no. 4, pp. 739–743, 2018.

[3] B. K. Post *et al.*, “Using Big Area Additive Manufacturing to directly manufacture a boat hull mould,” *Virtual Phys. Prototyp.*, vol. 14, no. 2, pp. 123– 129, 2019.

[4] K. M. M. Billah, J. L. Corone, M. C. Halbig, R. B. Wicker, and D. Espalin, “Electrical and Thermal Characterization of 3D Printed Thermoplastic Parts with Embedded Wires for High Current-Carrying Applications,” *IEEE Access*, vol. 7, pp. 1–1, 2019.

[5] J. L. C. Jr, K. M. Billah, C. F. A. Carrasco, S. A. Barraza, R. B. Wicker, and D. Espalin, “Hybrid Manufacturing with FDM Technology for Enabling Power Electronics Component Fabrication,” *Solid Free. Fabr. 2018*, no. August, pp. 357–364, 2018.

[6] A. A. Hassen, J. Lindahl, X. Chen, B. Post, L. Love, and V. Kunc, “Additive manufacturing of composite tooling using high temperature thermoplastic materials,” *Int. SAMPE Tech. Conf.*, vol. 2016-Janua, no. April 2018, 2016.

[7] X. Wang, M. Jiang, Z. Zhou, J. Gou, and D. Hui, “3D printing of polymer matrix composites: A review and prospective,” *Compos. Part B Eng.*, vol. 110, pp. 442– 458, 2017.

[8] A. A. Hassen *et al.*, “The durability of large-scale additive manufacturing composite molds,” in *CAMX Conference Proceedings, September 26-29, 2016.*, 2016, no. April 2018, pp. 0–10.

[9] Billah, K.M.M., Heineman, J., Mhatre, P., Roschli, A., Post, B., Kumar, V., Kim, S., Haye, G., Jackson, J., Skelton, Z. and Kunc, V., 2021. Large-scale additive manufacturing of self-heating molds. *Additive Manufacturing*, *47*, p.102282.

[10] C. Atkins *et al.*, “Wire Co-Extrusion With Big Area Additive Manufacturing,” in *Solid Freeform Fabrication 2019: Proceedings of the 30th Annual International*, 2019, pp. 1549–1557.

[11] S. Kim *et al.*, "Analysis on part distortion and residual stress in big area additive manufacturing with carbon fiber-reinforced thermoplastic using dehomogenization technique," *CAMX 2019 - Compos. Adv. Mater. Expo*, pp. 1–14, 2019.

[12] Pokkalla, D.K., Kumar, V., Jo, E., Hassen, A.A., Cakmak, E., Alwekar, S., Kunc, V., Vaidya, U., Baid, H.K. and Kim, S., 2022, April. Anisotropic mechanical properties of polymer composites from a hybrid additive manufacturing-compression molding process using x-ray computer tomography. In Nondestructive Characterization and Monitoring of Advanced Materials, Aerospace, Civil Infrastructure, and Transportation XVI (Vol. 12047, pp. 319-328). SPIE.

[13] Sharma, I., Kumar, P.D. and Maiti, P.R., 2015. The effect of fiber orientation and laminate layup on fiber-reinforced polymer composite. IUP Journal of Structural Engineering, 8(1), p.49.

[14] Kumar, P.D., Sharma, I. and Maiti, P.R., 2014. Parametric Study of a Simply Supported Composite Plate Using Finite Element Method. *i-Manager's Journal on Civil Engineering*, *4*(4), p.26.

[15] "NiChrome - Nickel Chromium Alloys." [Online]. Available: https://www.nickel-alloys.net/nickel_chrome_alloys.html. [Accessed: 11- May- 2020].

[16] "Heat capacities for some select substances." [Online]. Available: https://gchem.cm.utexas.edu/data/section2.php?target=heat-capacities.php. [Accessed: 04 – April 2022].

[17] Wang, Z.P. and Kumar, D., 2017. On the numerical implementation of continuous adjoint sensitivity for transient heat conduction problems using an isogeometric approach. Structural and Multidisciplinary Optimization, 56(2), pp.487-500.

[18]. Billah, K.M.M., Hassen, A.A., Nasirov, A., Haye, G., Heineman, J., Kunc, V. and Kim, S., 2020, November. Thermal Analysis of Large Area Additive Manufacturing Resistance Heating Composites for Out of Oven/Autoclave Applications. In *ASME International Mechanical Engineering Congress and Exposition* (Vol. 84485, p. V02AT02A040). American Society of Mechanical Engineers.

[19] Pokkalla, D.K., Wang, Z.P., Poh, L.H. and Quek, S.T., 2019. Isogeometric shape optimization of smoothed petal auxetics with prescribed nonlinear deformation. *Computer Methods in Applied Mechanics and Engineering*, *356*, pp.16-43.

[20] Pokkalla, D.K., Poh, L.H. and Quek, S.T., 2021. Isogeometric shape optimization of missing rib auxetics with prescribed negative Poisson's ratio over large strains using genetic algorithm. *International Journal of Mechanical Sciences*, *193*, p.106169.